

Supplemental information

**3D chromatin maps of the human pancreas
reveal lineage-specific regulatory
architecture of T2D risk**

Chun Su, Long Gao, Catherine L. May, James A. Pippin, Keith Boehm, Michelle Lee, Chengyang Liu, Matthew C. Pahl, Maria L. Golson, Ali Naji, HPAP Consortium, Struan F.A. Grant, Andrew D. Wells, and Klaus H. Kaestner

Supplemental Figure Legends

Supplemental Figure 1. Pancreatic islet cell transcriptomic profile defined using scRNA-seq. A, Clustering of gene expression profile from 5,288 pancreatic cells from organ donors without diabetes identified 9 distinct clusters on UMAP. Endo: endothelial; eps: epsilon (ghrelin producing); mes: mesenchymal; PP: (pancreatic polypeptide producing). B, the expression of marker genes in single cells and donor composition within cell type clusters. C, Pearson correlation of gene expression between donors. D, Pearson correlation of gene expression between cell types. E, Estimate of cell composition in sorted pancreatic cell subsets through integration of scRNA-seq. The cell type composition from bulk RNA-seq data on sorted pancreatic cell subsets were characterized using a list of gene markers obtained from panel B.

Supplemental Figure 2. Pancreatic islet cell chromatin accessibility profile defined using scATAC-seq. A, Clustering of accessible chromatin profile from 12,473 pancreatic cells from organ donors without diabetes identified 9 distinct clusters on UMAP. B, Promoter accessibility of selected marker genes in single cells and donor composition within cell type clusters. Promoters were defined as the window of -1,500 to +500bp around TSS in Gencode V19 annotation. C, scATAC-seq and bulk ATAC-seq accessibility signal around selected marker genes: CPA1 (acinar), GCG (alpha) and IGF2 (beta). Fragments were aggregated for each cell type in scATAC-seq. The coverage for both scATAC-seq and bulk ATAC-seq was normalized using the RPGC method from deeptools. D, Pearson correlation of OCR accessibility between scATAC-seq and bulk ATAC-seq. OCR accessibility were calculated as FPKM by mapping either cell type aggregated fragments from scATAC-seq or fragments of bulk ATAC-seq to the consensus pseudo-bulk peak reference. E, Spearman correlation between t-statistics of cluster-specific genes based on promoter accessibility (scATAC-seq) and gene expression (scRNA-seq).

Supplemental Figure 3. 3D chromatin architecture of pancreatic cell subsets defined by Hi-C assay. A, Stratum-adjusted correlation coefficient (SCC) between Hi-C samples to measure sample reproducibility and interrelationships of cell lineages. B, the number of Topologically Associating Domains (TADs) identified in each cell type. C, the distribution of TAD size in each cell type. D, Aggregate peak analysis (APA) plots of chromatin loops identified by the loop callers Mustache and Fit-Hi-C2. The APA scores were calculated with respect to the enrichment of the center pixel at 4kb resolution and labelled at the top left corner. E, Venn diagram of consensus loop calls across cell types. The consensus loops were collected by merging loop calls from 1kb, 2kb and 4kb resolutions with preference to keep the highest resolution data. F, The number of loops annotated to open chromatin regions (OCR) and genes. OCR (green): both anchors overlapped OCRs; Gene (teal): both anchors overlapped gene promoters (-1,500 to +500bp around the TSS). Gene-OCR (purple): one anchor overlapped an OCR and the other anchor overlapped a gene promoter. G, Z-score distribution of co-accessible promoters and distal OCRs detected by Hi-C chromatin loops. P-values were calculated by two-sided Wilcoxon rank sum test. H, The number of loop anchors overlapped with chromHMM chromatin features. chromHMM chromatin states for acinar and endocrine cells were previously defined in Arda et al. 2018. I, Enrichment of chromatin loops at open chromatin regions and regulatory chromatin

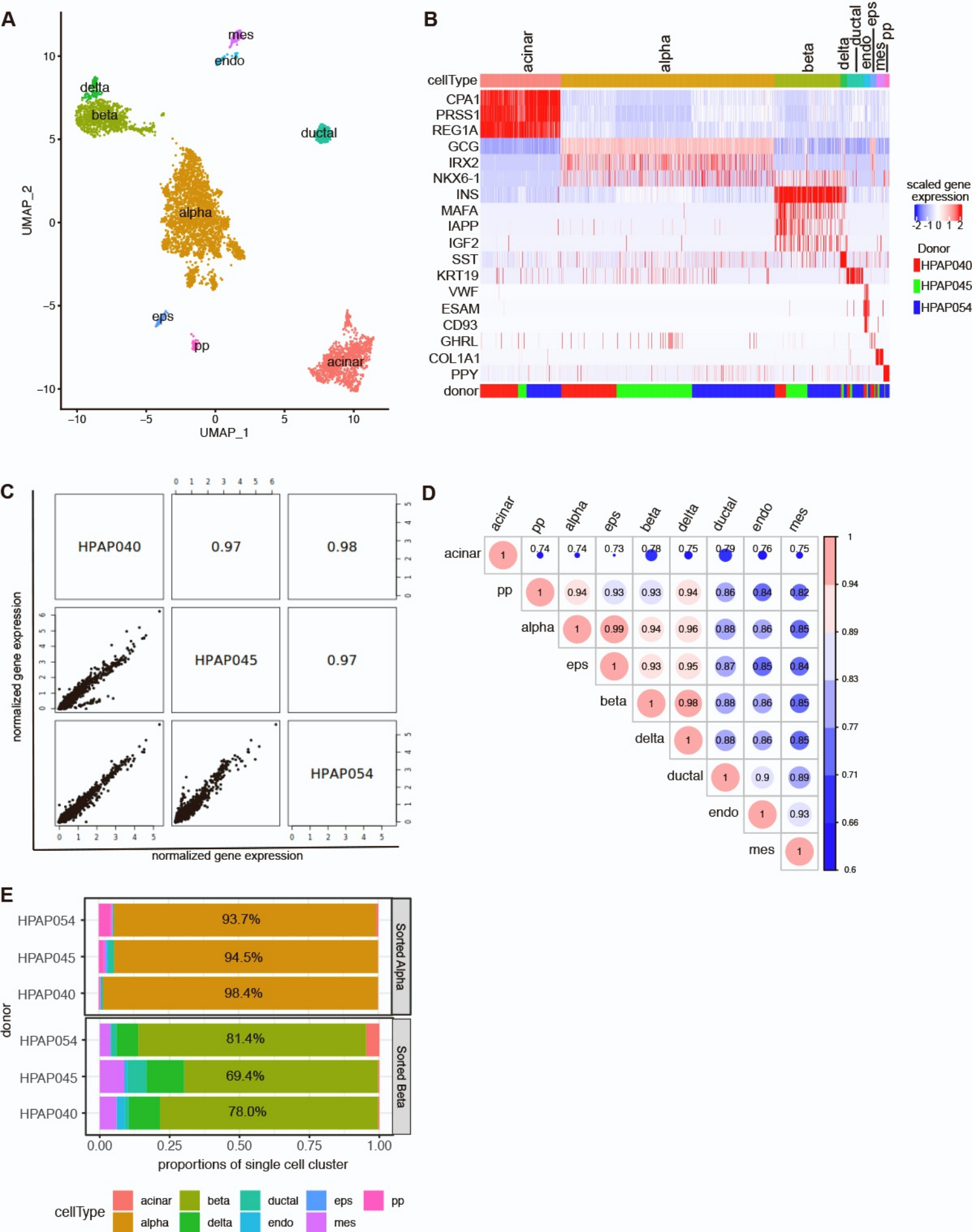
features defined by chromHMM. The enrichment fold change was obtained by comparing called loops to distance-matched random chromatin contacts. The p-value was calculated by a 100-fold permutation test.

Supplemental Figure 4. Illustration of variant-to-gene mapping. The candidate variants were first defined by proxy SNPs within high LD ($R^2 > 0.8$) with sentinel signals from GWAS, and then filtered to proxy SNPs located in open chromatin by peaks called from ATAC-seq. The open proxy SNPs were mapped to candidate genes with two approaches. (1) Distal genes were linked to open SNP-containing peaks with physical interaction evidence from Hi-C loop calls for each cell type (left diagram). (2) Proximal genes whose promoter regions (-1,500bp ~ +500bp of TSS) fall within open SNP-containing peaks.

Supplemental Figure 5. Cell type specific implicated genes and examples of likely disruption of transcription factor DNA binding motifs by T2D relevant SNPs. A. Comparison of genes implicated by our approach and that of Rai and colleagues (Rai et al., 2020). Yellow indicates sets of GWAS sentinel:gene pairs specific to this study, cyan indicates genes specific to Rai et al., 2020, and magenta indicates groups implicated in both studies. Sentinel:gene pairs specific to beta cells are highlighted (black: closest gene to sentinel, red not the closest gene). B. Genomic track for KCNQ1 a putative acinar cell specific effector gene. C. Variants at the TH/INS/TRPM5 locus that are in contact loops with the INS or TRPM5 promoter likely disrupt binding of the TFs indicated. D. Disruption of a putative NEUROD2 binding site by rs4234731 in the WSF1 gene. E. Genomic track for DGKB a putative beta cell specific effector gene.

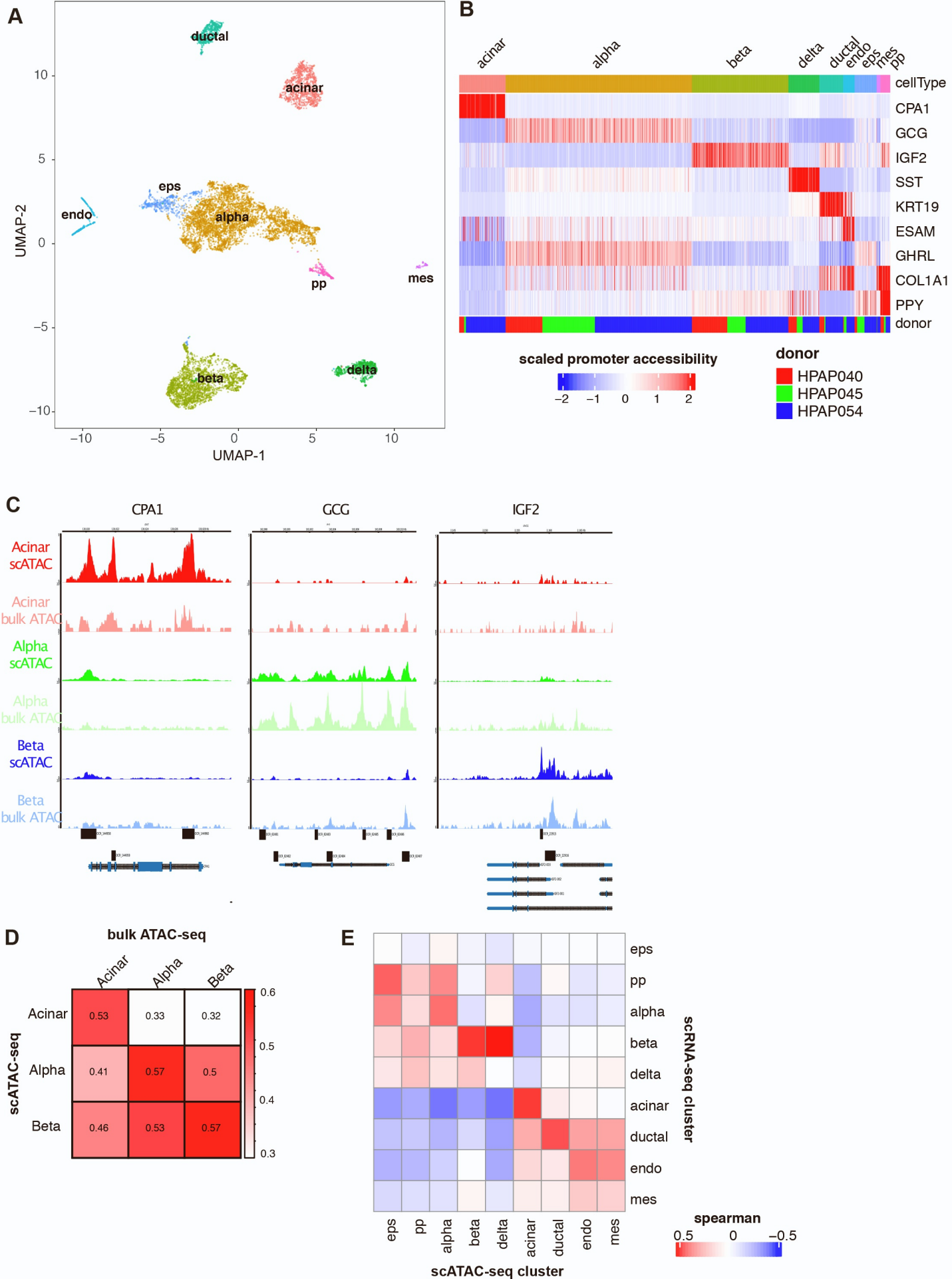
Supplemental Figure 6. Comparison of T2D variant-to-gene mapping with other diabetes relevant traits. A, ‘Upset’ plot of putative causal-variant-gene pairs across diabetes-related traits. Examined traits include type 2 diabetes (T2D), fasting glucose (FG), Hemoglobin A1C (HbA1c), fasting insulin (FI), 2h glucose (2hGlu) and T1D. Each row corresponds to the set of putative causal-variant to gene pairs in each trait. Each column corresponds to one segment of a Venn diagram obtained by intersecting the traits indicated as black circles. All segments that intersect with T2D are highlighted in red. The number of putative causal-variant to gene pairs in each set and intersecting segment are summarized in the bar graph on top. B, Stacked association plots of T2D with FG and HbA1c at T2D sentinel signal rs10228066. Variant-to-gene mapping implicates rs10228796 as the candidate causal variant and the linked rs10228796 to the candidate effector gene DGKB with beta cell-specific chromatin loops (Supplemental Figure 9C, Supplemental Table 10). C, HyPrColoc identified rs10228796 as a candidate causal variant explaining the shared association signal among T2D, FG and HbA1c. The posterior probability of colocalization between the traits was 0.819 and rs10228796 explained 33.6% of their colocalization.

Supplemental Figure 1. Single Cell RNAseq Analysis. Related to Figure 1.

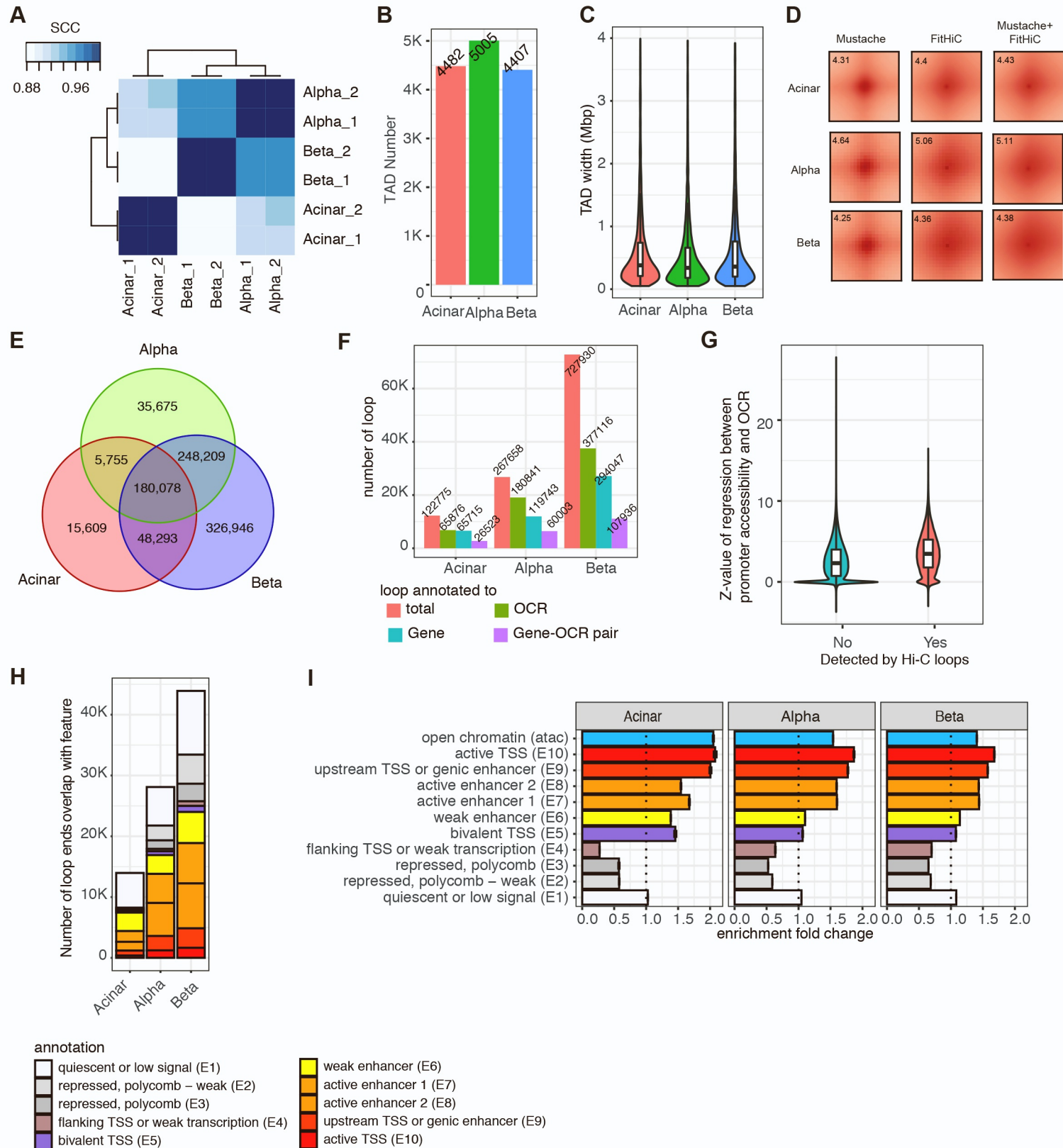


Supplemental Figure 2. Single Cell Chromatin Accessibility.

Related to Figures 2 and 3.

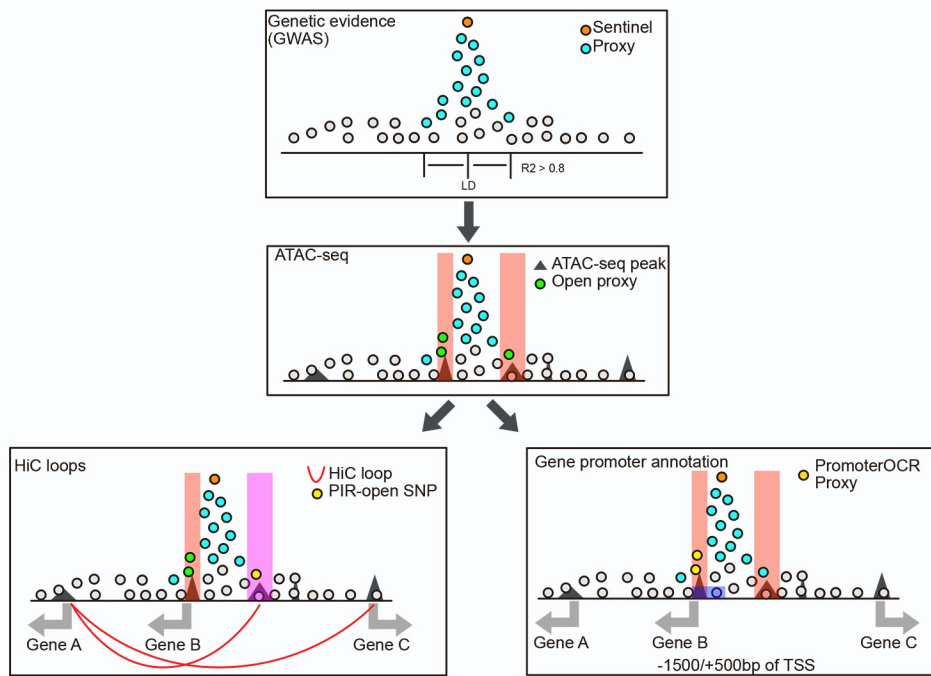


Supplemental Figure 3. Chromatin Loop Analysis. Related to Figure 3.

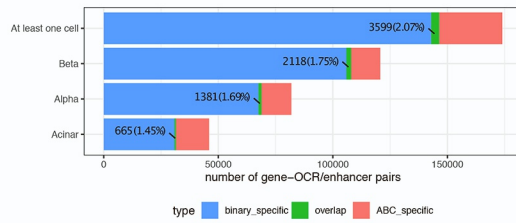


Supplemental Figure 4. Variant to Gene Mapping. Related to Figures 5 and 6.

A



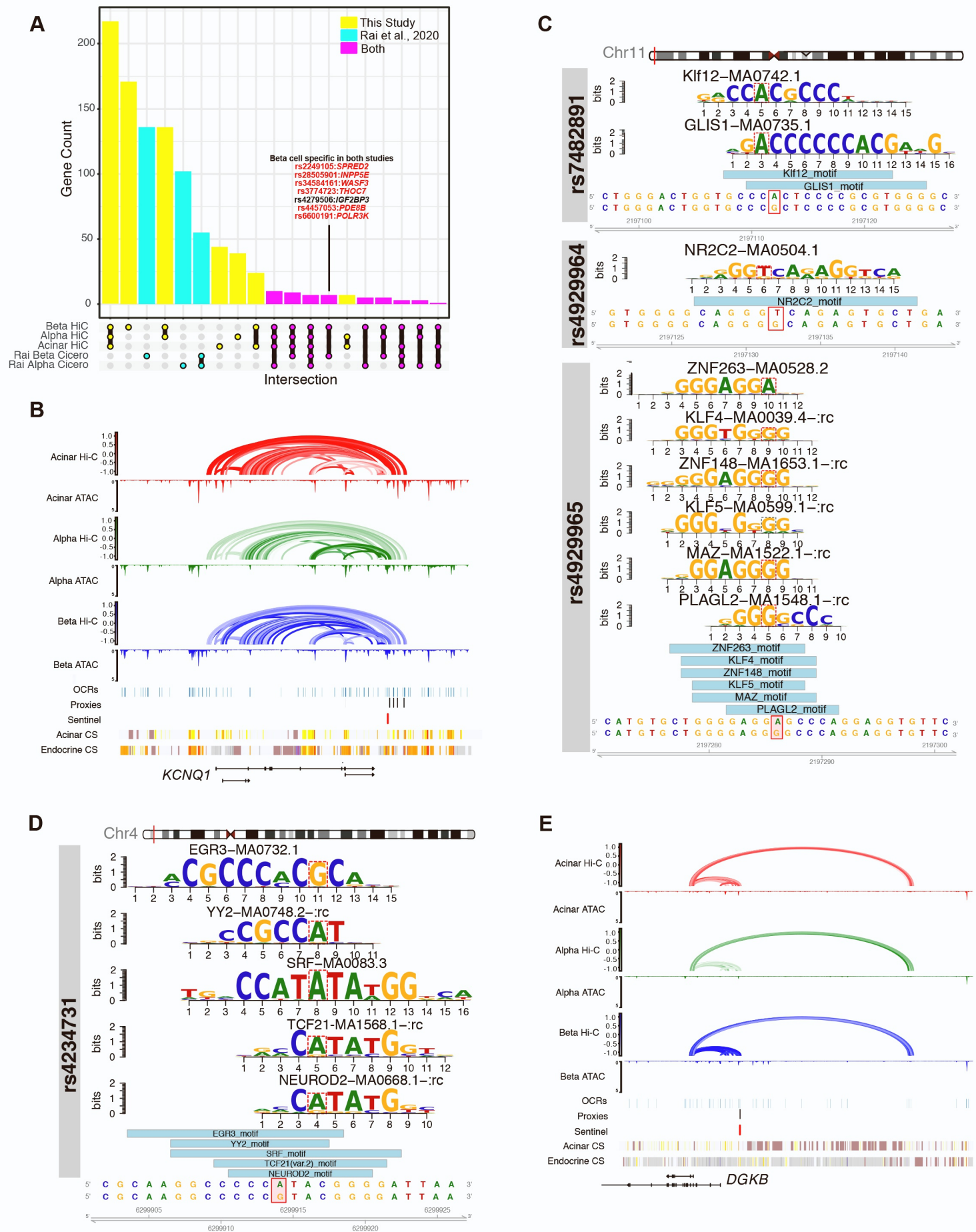
B



C

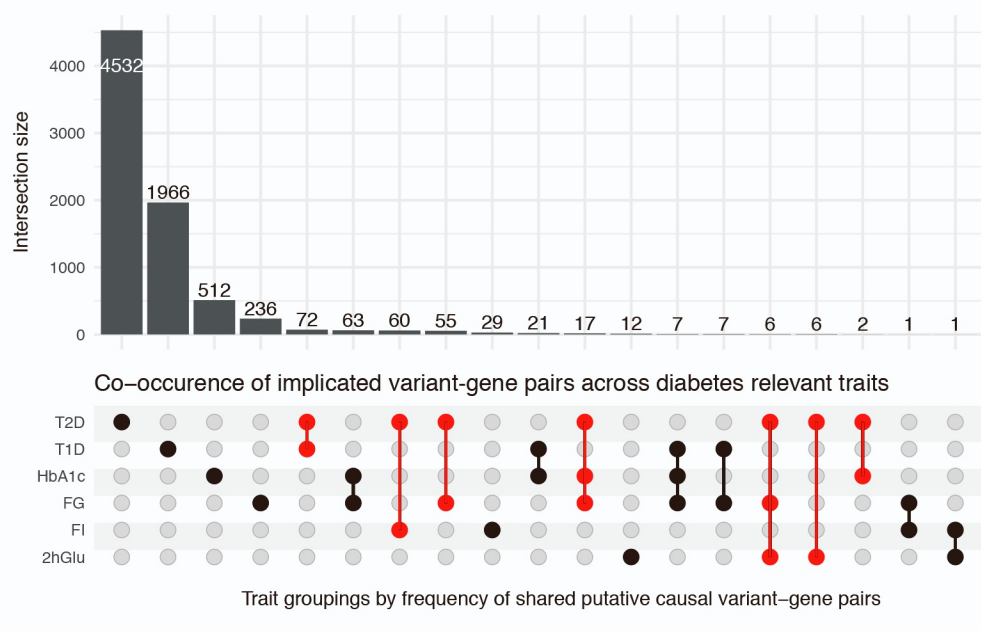


Supplemental Figure 5. Cell Type Specific Variant to Gene Mapping. Related to Figures 5 and 6.

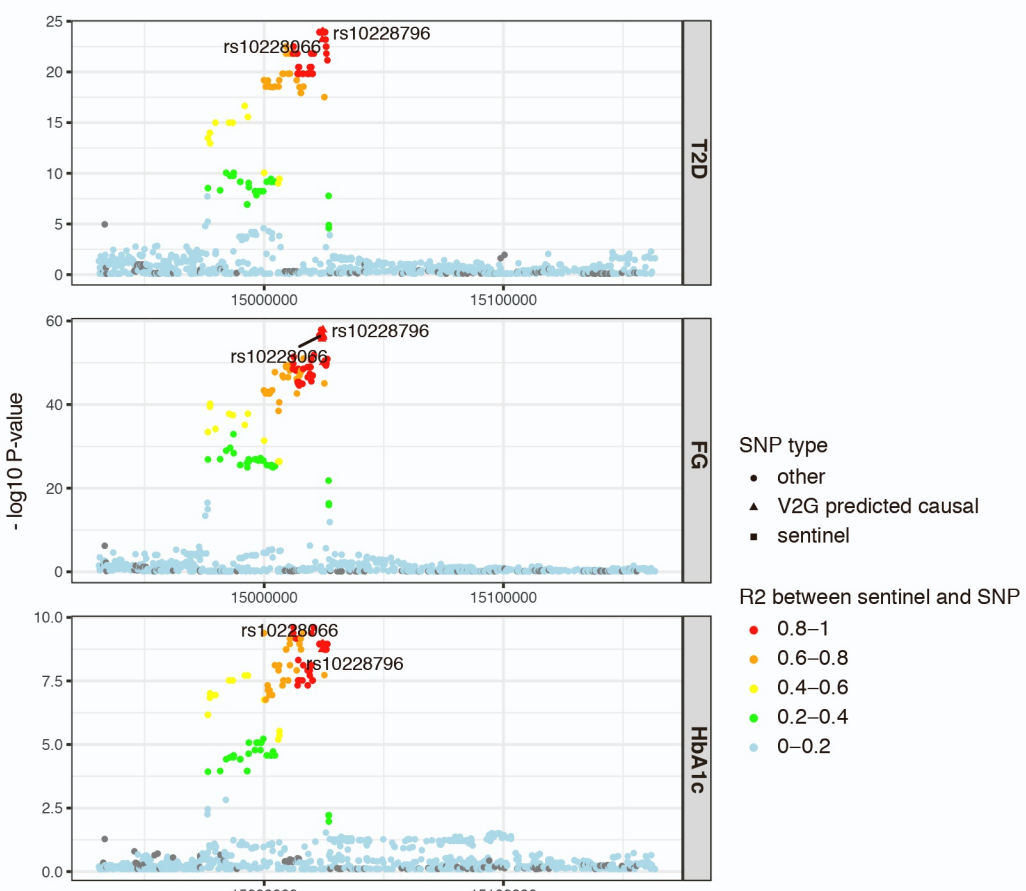


Supplemental Figure 6. Co-Occurance of variant-to-gene pairs. Related to Figures 5 and 6.

A.



B.



C.

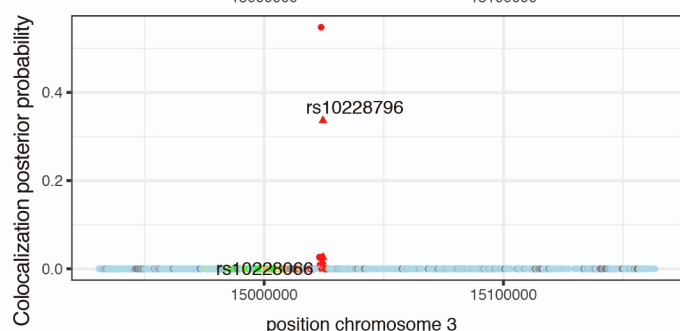


Table S1. Donor Information. Related to Figure 1.

Pancreata from non-diabetic organ donors were collected via the HPAP program and processed for the methodologies indicated.

technique	donor	Age	Sex	BMI	cell number	after filter
scRNA	HPAP040	35	M	23.98	2533	1519
scRNA	HPAP045	27	F	26.2	3744	1480
scRNA	HPAP054	40	F	30.85	2823	2289
bulkRNAseq	HPAP040	35	M	23.98	N/A	N/A
bulkRNAseq	HPAP045	27	F	26.2	N/A	N/A
bulkRNAseq	HPAP054	40	F	30.85	N/A	N/A
scATAC	HPAP040	35	M	23.98	4029	2653
scATAC	HPAP045	27	F	26.2	6093	3308
scATAC	HPAP054	40	F	30.85	7408	6512

technique	donor	Age	Sex	BMI	Cell Types analyzed
hi-C	HPAP040	35	M	23.98	acinar, alpha, beta
hi-C	HPAP045	27	F	26.2	alpha, beta
hi-C	HPAP054	40	F	30.85	acinar
hi-C	HPAP066	58	F	31.07	acinar, alpha, beta
hi-C	HPAP072	19	M	23.1	acinar

Table S2. Summary data for the HiC studies. Related to Figures 1 and 2.

sample	path	input #
Acinar_1_HiC	/mnt/isilon/sfgi/suc1/analyses/grant/hiC/hicup/Acinar_1/hicup/Acinar_1_hicupSummary.txt	2,712,288,871
Acinar_2_HiC	/mnt/isilon/sfgi/suc1/analyses/grant/hiC/hicup/Acinar_2/hicup/Acinar_2_hicupSummary.txt	3,249,462,125
Alpha_1_HiC	/mnt/isilon/sfgi/suc1/analyses/grant/hiC/hicup/Alpha_1/hicup/Alpha_1_hicupSummary.txt	3,471,287,075
Alpha_2_HiC	/mnt/isilon/sfgi/suc1/analyses/grant/hiC/hicup/Alpha_2/hicup/Alpha_2_hicupSummary.txt	2,269,661,813
Beta_1_HiC	/mnt/isilon/sfgi/suc1/analyses/grant/hiC/hicup/Beta_1/hicup/Beta_1_hicupSummary.txt	4,372,601,515
Beta_2_HiC	/mnt/isilon/sfgi/suc1/analyses/grant/hiC/hicup/Beta_2/hicup/Beta_2_hicupSummary.txt	4,693,960,014
Mean		

paired_align #	paired_align	valid_pair #	valid_pair %	same_circularised %	same_dangling_ends %	same_internal %
1,792,267,263	66.08	1,759,335,474	98.16	0.01	0.17	0.3
2,157,447,639	66.39	2,120,779,052	98.3	0.01	0.14	0.27
2,243,257,365	64.62	2,197,350,825	97.95	0.01	0.15	0.32
1,489,241,307	65.62	1,461,577,468	98.14	0.01	0.16	0.31
2,840,479,211	64.96	2,779,936,755	97.87	0.06	0.2	0.41
3,060,110,306	65.19	2,994,589,705	97.86	0.06	0.2	0.42

religation %	contiguous_sequence %	wrong_size %	unique_ditag #	unique_ditag %	usage efficiency
1.35	0	0	1,504,597,088	85.52	55.47%
1.27	0	0	1,776,039,581	83.74	54.66%
1.56	0	0	1,805,610,570	82.17	52.02%
1.37	0	0	1,232,759,953	84.34	54.31%
1.46	0	0	2,196,100,542	79	50.22%
1.46	0	0	2,316,680,304	77.36	49.35%
			1,805,298,006		

Table S3. Summary of Loop Calling from HiC data. Related to Figures 2 and 3.

file

/mnt/isilon/sfgi/suc1/analyses/grant/hiC/juicer/Acinar_2reps/hic_loops/all/Acinar_2reps.fithic_FDR.fdr1e6.res1000.bedpe
/mnt/isilon/sfgi/suc1/analyses/grant/hiC/juicer/Acinar_2reps/hic_loops/all/Acinar_2reps.mustache.pt01.res1000.bedpe
/mnt/isilon/sfgi/suc1/analyses/grant/hiC/juicer/Alpha_2reps/hic_loops/all/Alpha_2reps.fithic_FDR.fdr1e6.res1000.bedpe
/mnt/isilon/sfgi/suc1/analyses/grant/hiC/juicer/Alpha_2reps/hic_loops/all/Alpha_2reps.mustache.pt01.res1000.bedpe
/mnt/isilon/sfgi/suc1/analyses/grant/hiC/juicer/Beta_2reps/hic_loops/all/Beta_2reps.fithic_FDR.fdr1e6.res1000.bedpe
/mnt/isilon/sfgi/suc1/analyses/grant/hiC/juicer/Beta_2reps/hic_loops/all/Beta_2reps.mustache.pt01.res1000.bedpe

/mnt/isilon/sfgi/suc1/analyses/grant/hiC/juicer/Acinar_2reps/hic_loops/all/Acinar_2reps.fithic_FDR.fdr1e6.res2000.bedpe
/mnt/isilon/sfgi/suc1/analyses/grant/hiC/juicer/Acinar_2reps/hic_loops/all/Acinar_2reps.mustache.pt01.res2000.bedpe
/mnt/isilon/sfgi/suc1/analyses/grant/hiC/juicer/Alpha_2reps/hic_loops/all/Alpha_2reps.fithic_FDR.fdr1e6.res2000.bedpe
/mnt/isilon/sfgi/suc1/analyses/grant/hiC/juicer/Alpha_2reps/hic_loops/all/Alpha_2reps.mustache.pt01.res2000.bedpe
/mnt/isilon/sfgi/suc1/analyses/grant/hiC/juicer/Beta_2reps/hic_loops/all/Beta_2reps.fithic_FDR.fdr1e6.res2000.bedpe
/mnt/isilon/sfgi/suc1/analyses/grant/hiC/juicer/Beta_2reps/hic_loops/all/Beta_2reps.mustache.pt01.res2000.bedpe

/mnt/isilon/sfgi/suc1/analyses/grant/hiC/juicer/Acinar_2reps/hic_loops/all/Acinar_2reps.fithic_FDR.fdr1e6.res4000.bedpe
/mnt/isilon/sfgi/suc1/analyses/grant/hiC/juicer/Acinar_2reps/hic_loops/all/Acinar_2reps.mustache.pt01.res4000.bedpe
/mnt/isilon/sfgi/suc1/analyses/grant/hiC/juicer/Alpha_2reps/hic_loops/all/Alpha_2reps.fithic_FDR.fdr1e6.res4000.bedpe
/mnt/isilon/sfgi/suc1/analyses/grant/hiC/juicer/Alpha_2reps/hic_loops/all/Alpha_2reps.mustache.pt01.res4000.bedpe
/mnt/isilon/sfgi/suc1/analyses/grant/hiC/juicer/Beta_2reps/hic_loops/all/Beta_2reps.fithic_FDR.fdr1e6.res4000.bedpe
/mnt/isilon/sfgi/suc1/analyses/grant/hiC/juicer/Beta_2reps/hic_loops/all/Beta_2reps.mustache.pt01.res4000.bedpe

cell	loop caller	cutoff	resolution	total_LoopN	merge_caller
Acinar_2reps	fithic_FDR	fdr < 1e-6	res1000	90	
Acinar_2reps	mustache	pt < 0.1	res1000	536	626
Alpha_2reps	fithic_FDR	fdr < 1e-6	res1000	369	
Alpha_2reps	mustache	pt < 0.1	res1000	823	1,191
Beta_2reps	fithic_FDR	fdr < 1e-6	res1000	2,657	
Beta_2reps	mustache	pt < 0.1	res1000	3,241	5,862
Acinar_2reps	fithic_FDR	fdr < 1e-6	res2000	7,565	
Acinar_2reps	mustache	pt < 0.1	res2000	5,206	12,542
Alpha_2reps	fithic_FDR	fdr < 1e-6	res2000	21,760	
Alpha_2reps	mustache	pt < 0.1	res2000	9,055	30,263
Beta_2reps	fithic_FDR	fdr < 1e-6	res2000	100,331	
Beta_2reps	mustache	pt < 0.1	res2000	17,300	115,935
Acinar_2reps	fithic_FDR	fdr < 1e-6	res4000	124,634	
Acinar_2reps	mustache	pt < 0.1	res4000	10,524	132,603
Alpha_2reps	fithic_FDR	fdr < 1e-6	res4000	278,357	
Alpha_2reps	mustache	pt < 0.1	res4000	17,656	291,377
Beta_2reps	fithic_FDR	fdr < 1e-6	res4000	781,486	
Beta_2reps	mustache	pt < 0.1	res4000	25,069	797,482

consensus loops within resolution **final consensus loops across cells** **consensus loops at each resolution**

7,499

7,499

142,709

129,492

938,900

860,565

723,574

Table S4: Gene Ontology Analysis. Related to Figures 2 and 3.

gene set	pathway	fdr	pathway_ger observed	genes
endocrine-specific genes	enteroendocrine_cell_differentiation	0.01238328	28	8 PAX6,RFX3,GSK3B,CDK6,BMP5,NEUROD1,NKX6-1,INSM1
endocrine-specific genes	glandular_epithelial_cell_development	0.02841586	25	7 PAX6,RFX3,GSK3B,CDK6,BMP5,NKX6-1,INSM1
endocrine-specific genes	columnar_cuboidal_epithelial_cell_development	0.02841586	58	10 PAX6,RFX3,GSK3B,HIF1A,CDK6,C1GALT1,NKX3-2,BMP5,NKX6-1,INSM1
endocrine-specific genes	type_b_pancreatic_cell_development	0.04452176	20	6 RFX3,GSK3B,CDK6,BMP5,NKX6-1,INSM1
endocrine-specific genes	pancreas_development	0.04452176	78	11 PAX6,ISL1,RFX3,GSK3B,CDK6,NKX3-2,BMP5,MEIS2,NEUROD1,NKX6-1,INSM1
endocrine-specific genes	endocrine_pancreas_development	0.09101823	45	8 PAX6,RFX3,GSK3B,CDK6,BMP5,NEUROD1,NKX6-1,INSM1
acinar-specific genes	isoprenoid_metabolic_process	4.38E-04	139	17 DPM1,CYP26B1,AKR1B1,SDC4,APOE,CYP2E1,CYP1B1,CYP2C8,RBP4,
acinar-specific genes	terpenoid_metabolic_process	4.38E-04	120	16 CYP26B1,AKR1B1,SDC4,APOE,CYP2E1,CYP1B1,CYP2C8,RBP4,RLBP1
acinar-specific genes	dna_binding_transcription_factor_activity_rna_polymerase_ii_specific	4.38E-04	1094	59 ZBTB32,BARX2,FOXC1,SP100,PAX2,REST,IKZF5,VSX1,ADNP,TCFL5,INR113,VAX1,NKX6-2,HHEX,ERG,ETS2,TAL1,FOXQ1,NKX3-1,HOXD4,;9 AKR1B1,CYP1B1,CYP2C8,RBP4,DHRS3,ALDH1A3,CYP27C1,ADH7,AKI11 CYP26B1,AFM,AFP,APOC1,S100A8,S100A9,ALB,FFAR4,CYP27C1,SE48 ZBTB32,BARX2,FOXC1,MCM10,PAX2,REST,IKZF5,TCFL5,ETV2,EBF3FOXF2,SMAD6,NR113,VAX1,NKX6-2,HHEX,ERG,ETS2,TAL1,FOXQ1,NR0046,AFM,AFP,APOC1,S100A8,S100A9,ALB,FFAR4,UGT1A814 CYP26B1,AFP,REST,AKR1B1,CYP1B1,CYP2C8,RBP4,DHRS3,UGT2B717 BIRC5,SERPINA4,AVP,WFDC2,KNG1,HRG,SLPI,WFDC3,ADRM1,NGF49 ZBTB32,BARX2,FOXC1,MCM10,PAX2,REST,IKZF5,TCFL5,ETV2,EBF3VAX1,NKX6-2,HHEX,ERG,ETS2,TAL1,FOXQ1,NKX3-1,HOXD4,NHLH1,48 ZBTB32,BARX2,FOXC1,PAX2,REST,IKZF5,VSX1,TCFL5,ETV2,EBF3,N,SMAD6,NR113,VAX1,NKX6-2,HHEX,ERG,ETS2,TAL1,FOXQ1,NKX3-1,61 ZBTB32,BARX2,FOXC1,SP100,PAX2,SP140,REST,IKZF5,VSX1,ADNP,MAD6,ZNF287,NR113,VAX1,NKX6-2,HHEX,ERG,ETS2,TAL1,FOXQ1,NR35 PAX2,REST,TCFL5,ETV2,EBF3,NANOG,RFX4,KCNIP3,VAX2,MYB,RBF11 REST,AKR1B1,CYP1B1,CYP2C8,RBP4,ACSS1,DHRS3,ALDH1A3,CYP27B718 BIRC5,SERPINA4,AVP,WFDC2,KNG1,HRG,SLPI,WFDC3,ADRM1,NGF11 SERPINA4,WFDC2,HRG,SLPI,WFDC3,COL6A3,SERPINA11,SERPINA5,26 LAMA3,FGFR2,COL4A4,ICAM1,ITGA6,COL9A3,GDF10,SMOC2,KNG5 TMC5,TMC6,PIEZ02,TMC8,TMC719 ZBTB32,REST,IKZF5,TCFL5,KCNIP3,VAX2,GZF1,GSC,MYC,VAX1,NKX31 FGFR2,PAX2,EDN1,DNMT3B,ICAM1,AVP,OXT,USP46,APOBEC1,MYI7 CYP26B1,RBP4,RLBP1,CYP27C1,SERPINA5,ADH7,UGT1A854 ZBTB32,BARX2,FOXC1,MCM10,PAX2,REST,IKZF5,VSX1,TCFL5,ETV2FOXF2,SMAD6,NR113,VAX1,NKX6-2,HHEX,ERG,ETS2,TAL1,FOXQ1,NR5 PAX2,HOXB2,KCN2A2,DLL1,PLXNA424 BIRC5,SERPINA4,AVP,WFDC2,PHACTR1,KNG1,HRG,SLPI,WFDC3,AF27 PDCC2,PAX2,REST,BIRC5,SERPINA4,AVP,CSNK2A1,WFDC2,KNG1,H11 ICAM1,PIK3CG,IL1B,SAA2,S100A8,AHSG,OSMR,SAA4,IL31RA,CEBPI52 SP100,PAX2,ARHGAP28,FKBP1A,BIRC5,SERPINA4,ADNP,AVP,CSNKYSF,CYP1B1,AHSG,EPHA1,COMM7,LYPD1,MGAT5,HHEX,OXA1L,SH4 PAX2,HOXB2,KCN2A2,PLXNA46 CYP26B1,CYP2C8,ALDH1A3,CYP27C1,ADH7,UGT1A860 LAMA3,LIMS2,ADD2,ICAM3,ICAM1,ITGA6,TM9SF4,ICAM4,ICAM5,P,SMAD6,CYP1B1,CUZD1,ENTPD1,FBLN5,S100A8,ACKR3,ITGA9,EPH,55 ZBTB32,BARX2,FOXC1,MCM10,SP100,PAX2,BIRC5,VSX1,ADNP,TCFSMAD6,NR113,VAX1,NKX6-2,HHEX,ERG,ETS2,TAL1,FOXQ1,NKX3-1,7 TCHH,SPRR1B,SPRR1A,KAZN,HRNR,SPRR2A,SPRR2F25 BARX2,FOXC1,ETV2,EBF3,NANOG,RFX4,MYB,RBPJL,HOXD3,MYC,IF
acinar-specific genes	retinol_metabolic_process	0.00273548	44	
acinar-specific genes	monocarboxylic_acid_binding	0.00273548	68	
acinar-specific genes	sequence_specific_double_stranded_dna_binding	0.00273548	889	
acinar-specific genes	fatty_acid_binding	0.0046275	36	
acinar-specific genes	cellular_hormone_metabolic_process	0.00856178	130	
acinar-specific genes	endopeptidase_regulator_activity	0.00856178	185	
acinar-specific genes	double_stranded_dna_binding	0.00972106	981	
acinar-specific genes	regulatory_region_nucleic_acid_binding	0.00994444	960	
acinar-specific genes	dna_binding_transcription_factor_activity	0.00994444	1334	
acinar-specific genes	cis regulatory_region_binding	0.0110201	616	
acinar-specific genes	primary_alcohol_metabolic_process	0.01419379	89	
acinar-specific genes	peptidase_regulator_activity	0.0148747	222	
acinar-specific genes	serine_type_endopeptidase_inhibitor_activity	0.01607133	92	
acinar-specific genes	collagen-containing_extracellular_matrix	0.01607133	408	
acinar-specific genes	mechanosensitiveIon_channel_activity	0.01607133	15	
acinar-specific genes	dna_binding_transcription_repressor_activity	0.01629605	249	
acinar-specific genes	response_to_toxic_substance	0.0168696	539	
acinar-specific genes	isoprenoid_binding	0.0168696	36	
acinar-specific genes	sequence_specific_dna_binding	0.02164157	1189	
acinar-specific genes	anatomical_structure_arrangement	0.02482279	17	
acinar-specific genes	enzyme_inhibitor_activity	0.02495516	378	
acinar-specific genes	regulation_of_peptidase_activity	0.02682114	455	
acinar-specific genes	acute_inflammatory_response	0.04717984	109	
acinar-specific genes	negative_regulation_of_molecular_function	0.04717984	1174	
acinar-specific genes	cranial_nerve_structural_organization	0.04717984	11	
acinar-specific genes	retinoic_acid_metabolic_process	0.04757557	32	
acinar-specific genes	biological_adhesion	0.04757557	1425	
acinar-specific genes	nuclear_chromosome	0.04757557	1273	
acinar-specific genes	cornified_envelope	0.04757557	45	
acinar-specific genes	dna_binding_transcription_activator_activity	0.04757557	427	

;M1

5-1,INSM1

,RLBP1,DHRS3,PNLIP,ALDH1A3,CYP27C1,ADH7,AKR1B10,UGT1A8

,DHR53,PNLIP,ALDH1A3,CYP27C1,ADH7,AKR1B10,UGT1A8

ETV2,EBF3,NANOG,RFX4,IRX4,KCNIP3,VAX2,MYB,RBPJL,FOXA2,GZF1,HOXD1,HOXD3,GSC,SP110,MYC,IRF4,FOXF2,SMAD6,

ZNF524,NHLH1,ZNF217,CEPB,HOXB2,HOXD8,TGIF1,NHLH2,SOX12,FOX51,FIGLA,SP140L,FOXD2,FOXE3,LITAF,ZNF580,HMX1,ZGLP1,EBF2,ASCL5

R1B10

SERPIN A5,UGT1A8

,NANOG,RFX4,KCNIP3,VAX2,MYB,RBPJL,FOXA2,GZF1,HOXD3,GSC,MYC,IRF4,

NKX3-1,HOXD4,NHLH1,ZNF217,CEPB,HOXB2,HOXD8,TGIF1,NHLH2,SOX12,FOX51,FIGLA,LITAF,HMX1,EBF2,ASCL5

,ALDH1A3,CYP27C1,ADH7,AKR1B10,UGT1A8

,AHSG,COL6A3,SERPINA11,SERPINA5,SERPINA3,SPINK14,SPINK9

,NANOG,RFX4,KCNIP3,VAX2,MYB,RBPJL,FOXA2,GZF1,HOXD3,GSC,MYC,IRF4,FOXF2,SMAD6,NR1I3,

ZNF217,CEPB,HOXB2,HOXD8,TGIF1,NHLH2,SOX12,ZCCHC3,FOX51,FIGLA,LITAF,HMX1,EBF2,ASCL5

ANOG,RFX4,KCNIP3,VAX2,MYB,RBPJL,FOXA2,GZF1,HOXD3,GSC,MYC,IRF4,FOXF2,

HOXD4,NHLH1,ZNF217,CEPB,HOXB2,HOXD8,TGIF1,NHLH2,SOX12,FOX51,FIGLA,LITAF,HMX1,EBF2,ASCL5

TCFL5,ETV2,EBF3,NANOG,RFX4,IRX4,KCNIP3,VAX2,MYB,RBPJL,FOXA2,GZF1,HOXD1,HOXD3,GSC,SP110,MYC,IRF4,FOXF2,S5

NKX3-1,HOXD4,ZNF524,NHLH1,ZNF217,CEPB,HOXB2,HOXD8,TGIF1,NHLH2,SOX12,FOX51,FIGLA,SP140L,FOXD2,FOXE3,LITAF,ZNF580,HMX1,ZGLP1,EBF2,ASCL5

PJL,FOXA2,GZF1,HOXD3,GSC,MYC,IRF4,SMAD6,VAX1,NKX6-2,HHEX,ERG,ETS2,TAL1,FOXQ1,NKX3-1,ZNF217,CEPB,HOXB2,TGIF1,NHLH2,FOX51,FIGLA,LITAF,EBF2

7C1,ADH7,AKR1B10

,AHSG,COL6A3,NKX3-1,SERPINA11,SERPINA5,SERPINA3,SPINK14,SPINK9

,SERPINA3,SPINK14,SPINK9

1,HRG,SLPI,MATN4,APOE,ADAMDEC1,FBLN5,S100A8,AHSG,LAD1,S100A9,COL6A3,HTRA1,THBS2,SERPINA5,SERPINA3,COL13A1,HRNR

6-2,HHEX,ETS2,FOXQ1,ZNF217,CEPB,TGIF1,FOX51,HMX1

B,MPST,APOE,CYP2E1,TLR2,CYP1B1,RBP4,FBLN5,S100A8,RGS10,LYPD1,S100A9,ALB,GPX8,BCL2L1,ADH7,ADA,GSTK1,AKR1B10,ZNF580,INMT,SRXN1

,EBF3,NANOG,RFX4,IRX4,KCNIP3,VAX2,MYB,RBPJL,FOXA2,GZF1,HOXD1,HOXD3,GSC,MYC,IRF4,

NKX3-1,HOXD4,NHLH1,ZNF217,CEPB,HOXB2,HOXD8,TGIF1,NHLH2,SOX12,FOX51,FIGLA,FOXD2,FOXE3,LITAF,HMX1,ZGLP1,EBF2,ASCL5

POC1,NGF,AHSG,MGAT5,SH3RF2,COL6A3,SOCS3,SERPINA11,SERPINA5,SERPINA3,SPINK14,SPINK9,FGFR1OP,UGT1A8,PINX1

RG,SLPI,WFDC3,ADRM1,NGF,MYC,S100A8,AHSG,S100A9,COL6A3,NKX3-1,MALT1,CASC2,SERPINA11,SERPINA5,SERPINA3,SPINK14,SPINK9

B,SERPINA3

2A1,WFDC2,MAPK8,PHACTR1,DUSP22,KNG1,HRG,TNNT2,SLPI,WFDC3,IL1B,FOXA2,SH3BP4,APOE,APOC1,NGF,D

-3RF2,COL6A3,NKX3-1,TMC8,FOX51,KCNE1,SOCS3,SERPINA11,SERPINA5,SERPINA3,ADH7,PTPN1,SPINK14,SPINK9,FGFR1OP,UGT1A8,DBNDD2,PINX1,MTRNR2L6

IK3CG,DOCK8,CDH23,MAP3K8,SMOC2,DUSP22,KNG1,HRG,CD58,MYB,LY9,SDC4,IL1B,FOXA2,HOXD3,ADAMDEC1,VTCN1,DYSF,GPNMB,LRRK32L13A1,DLL1,PLXNA4,CLDN23

A1,DOCK5,HABP2,ADAM12,ROBO4,MPZ,ZYX,PDPN,INHBB,S100A9,COL6A3,DACT2,MALT1,CEPB,SLTRK1,THBS2,PEAR1,AJAP1,ADA,CO

L5,CSNK2A1,EBF3,NANOG,RFX4,IRX4,VAX2,TCP1,Lrif1,RBPJL,FOXA2,HOXD1,HOXD3,GSC,MYC,IRF4,FOXF2,

HOXD4,NHLH1,CEPB,HOXB2,HOXD8,TGIF1,NHLH2,SOX12,FOX51,FIGLA,SS18L1,FOXD2,FOXE3,HUS1B,ZNF580,HMX1,EBF2,ASCL5,PINX1

RF4,FOXF2,NR1I3,ERG,HOXD4,NHLH1,CEPB,HOXB2,HOXD8,NHLH2,SOX12,FIGLA,FOXD2,LITAF,EBF2

Table S8: Enrichment of diabetes-associated genetic risk variants by pancreatic cell type. Related to Figure 5.

Category	Prop._SNPs	Prop._h2	Prop._h2_std	Enrichment	Enrichment_	Enrichment_fdr
2hGlu.geneAnnotatedOCR_Acinar	0.00855617	0.16764967	0.07526909	19.5940009	8.79705077	0.03046446
2hGlu.geneAnnotatedOCR_Alpha	0.01260285	0.20947575	0.09461634	16.6213057	7.50753791	0.0312846
2hGlu.geneAnnotatedOCR_Beta	0.01366653	0.28189533	0.12457444	20.6267011	9.11529739	0.02708337
atrial_fibrillation.geneAnnotatedOCR_Acinar	0.00855617	-0.0070516	0.0450305	-0.8241541	5.26292515	0.72898969
atrial_fibrillation.geneAnnotatedOCR_Alpha	0.01260285	0.09509896	0.05563086	7.54583268	4.41415045	0.14614653
atrial_fibrillation.geneAnnotatedOCR_Beta	0.01366653	0.057474646	0.05133715	4.00588021	3.75641586	0.42721354
chronotype.geneAnnotatedOCR_Acinar	0.00855617	0.07281258	0.01755409	8.50994717	2.05162882	2.55E-04
chronotype.geneAnnotatedOCR_Alpha	0.01260285	0.10868292	0.02066125	8.62368097	1.63941184	3.91E-06
chronotype.geneAnnotatedOCR_Beta	0.01366653	0.13621118	0.02342549	9.96677503	1.71407767	2.70E-07
FG.geneAnnotatedOCR_Acinar	0.00855617	0.1483003	0.04462611	17.3325496	5.21566265	0.00300735
FG.geneAnnotatedOCR_Alpha	0.01260285	0.29933307	0.05645784	23.751229	4.47976917	1.05E-06
FG.geneAnnotatedOCR_Beta	0.01366653	0.47871629	0.10560444	35.0283845	7.72723414	2.27E-05
Fl.geneAnnotatedOCR_Acinar	0.00855617	0.0693239	0.03755978	8.102209	4.3897868	0.09839489
Fl.geneAnnotatedOCR_Alpha	0.01260285	0.06595173	0.03798391	5.23308231	3.01391524	0.15335084
Fl.geneAnnotatedOCR_Beta	0.01366653	0.03286877	0.03664848	2.40505679	2.68162407	0.59594923
HbA1c.geneAnnotatedOCR_Acinar	0.00855617	0.08464628	0.03668295	9.8930062	4.28730794	0.03437695
HbA1c.geneAnnotatedOCR_Alpha	0.01260285	0.10465562	0.04659651	8.30412647	3.6973009	0.04231339
HbA1c.geneAnnotatedOCR_Beta	0.01366653	0.18110832	0.05440388	13.251966	3.98081287	0.00154961
HOMA-B.geneAnnotatedOCR_Acinar	0.00855617	0.16305973	0.10297413	19.0575539	12.0350677	0.13426201
HOMA-B.geneAnnotatedOCR_Alpha	0.01260285	0.19825909	0.11325182	15.7312958	8.98621047	0.10037413
HOMA-B.geneAnnotatedOCR_Beta	0.01366653	0.36140907	0.14635052	26.4448399	10.7086856	0.01316583
HOMA-IR.geneAnnotatedOCR_Acinar	0.00855617	0.0581504	0.03252324	6.79630905	12.0676896	0.63298391
HOMA-IR.geneAnnotatedOCR_Alpha	0.01260285	0.07075903	0.11331771	0.60226895	8.99143833	0.96456976
HOMA-IR.geneAnnotatedOCR_Beta	0.01366653	0.09594914	0.11296438	7.02074139	8.26577164	0.46151987
pancCancer.Rashkin_NatComm2020.geneAnnotatedO	0.00855617	46.0254791	8688.73098	5379.21301	1015492.63	0.00160062
pancCancer.Rashkin_NatComm2020.geneAnnotatedO	0.01260285	10.1579979	408.855324	806.008272	32441.5084	0.03399007
pancCancer.Rashkin_NatComm2020.geneAnnotatedO	0.01366653	15.2616232	4391.98782	1116.71571	321368.293	0.03227247
sleepDuration_selfReported.geneAnnotatedOCR_Acin	0.00855617	0.04147672	0.01805838	4.84757856	2.11056685	0.0680744
sleepDuration_selfReported.geneAnnotatedOCR_Alph	0.01260285	0.07214588	0.02144071	5.72457076	1.70125906	0.00571416
sleepDuration_selfReported.geneAnnotatedOCR_Beta	0.01366653	0.10383472	0.02219802	7.59774116	1.62426238	6.89E-05
T1D.Chiou_Nat2021.geneAnnotatedOCR_Acinar	0.00855617	0.09903346	0.11180016	11.5745037	13.0666078	0.39971358
T1D.Chiou_Nat2021.geneAnnotatedOCR_Alpha	0.01260285	0.15989746	0.08853903	12.6874095	7.02532087	0.09145148
T1D.Chiou_Nat2021.geneAnnotatedOCR_Beta	0.01366653	0.19006722	0.11303459	13.9075018	8.27090954	0.11587556
T2D.Mahajan_NatGenet2018b.geneAnnotatedOCR_Ai	0.00855617	0.12327666	0.04235348	14.4079201	4.95004905	0.00754301
T2D.Mahajan_NatGenet2018b.geneAnnotatedOCR_Ai	0.01260285	0.17354021	0.05379666	13.7699228	4.26861178	0.00329411
T2D.Mahajan_NatGenet2018b.geneAnnotatedOCR_Bi	0.01366653	0.2331373	0.05792345	17.0590036	4.23834547	2.39E-04
						0.00740902

Table S14: Genetic variants with likely pleiotropic effects between T2D and glycemic traits. Related to Figures 5 and 6.

							ENSG000001TP53INP1
			rs7003387	chr8:959619:	0.020074	ENSG000001NDUFAF6	
						ENSG000002RP11-347C18.3	
						ENSG000001TP53INP1	
rs13024606	T2D, FI	0.9692	1 rs13389219	0.8018 rs7607980	chr2:165551:	1.71E-07	ENSG000001COBL1
rs1903002	T2D, FI	0.8956	0.9993 rs13133548	0.2781 rs13133548	chr4:897401:	0.27807708	ENSG000001FAM13A
							ENSG000002RP11-84C13.1
							ENSG000001TIGD2
rs9505097	FG, HbA1c	0.997	1 rs3778321	0.9996 rs76823979	chr6:723666:	3.07E-06	ENSG000002RP1-80N2.2
							ENSG000002RP1-80N2.3
							ENSG000002RP3-470L22.1
							ENSG000001RREB1
			rs17672741	chr6:723940:	4.21E-06	ENSG000002RP1-80N2.2	
						ENSG000002RP1-80N2.3	
						ENSG000002RP3-470L22.1	
						ENSG000001RREB1	